DOI 10.1007/s11141-016-9682-x
Radiophysics and Quantum Electronics, Vol. 59, No. 2, July, 2016
(Russian Original Vol. 59, No. 2, February, 2016)

THE ELECTRON-OPTICAL SYSTEM OF A GYROTRON WITH AN OPERATING FREQUENCY OF 263 GHz FOR SPECTROSCOPIC RESEARCH

A. N. Kuftin[1] **and V. N. Manuilov**[1,2*]

UDC 621.385.69

We describe specific features of modeling numerically the operation of magnetron-injection guns, which form high-quality helical electron beams in gyrotrons operated in the short-wave part of the millimeter-wave band (at a wavelength of 1 *mm). As an example, we consider the gun of a gyrotron having an operating frequency of* 263 *GHz designed for spectroscopic research. It is shown that there are good reasons to perform calculations and optimization of the magnetron-injection gun in two steps. At the first step, a simplest two-dimensional model can be used, which allows only for the influence of the field of the electrodes and the intrinsic space charge of the beam on the beam parameters. At the second, final stage one should allow for such factors as roughness of the emitting surface and thermal velocities of electrons. The electron distribution function in oscillatory velocities and the coefficient of electron reflection from the magnetic mirror should be calculated. It is demonstrated that the magnetron-injection gun, which is optimized by the method presented, is sufficiently universal and can be operated both at the first and second cyclotron-frequency harmonics. This opens up the possibility of developing gyrotrons for spectroscopy applications at frequencies of* 263 *and* 526 *GHz, respectively, which are required for biological and medical research.*

1. INTRODUCTION

The subterahertz frequency band (0.1–1.0 THz) has certain features, which make it very attractive for a wide range of fundamental and applied research in the fields of physics, chemistry, biology, and medicine. Sources of high-power (up to hundreds of kilowatts) radiation in the above-specified band can be used to produce dense plasma and control plasma parameters (controlled fusion), develop "point" plasma sources of X-ray radiation, and detect ionizing-radiation sources remotely [1, 2], as well as in many technological applications [3]. At a lower power (tens and hundreds of watts in the continuous regime), these sources are promising for diagnostics and spectroscopy of various media, including the methods of electron paramagnetic resonance and high-resolution nuclear magnetic resonance [4].

The most successful devices, which ensure the achievement of the above-specified power P and frequency f, are gyrotrons [5]. Specifically, gyrotrons for spectroscopy problems, which have the power $P \approx 50$–100 W and the frequency $f \approx 200$–300 GHz, have already been developed [6]. The achievable power level, as well as the capability of operating in the continuous regime with high stability of output parameters, which is required for spectroscopy, are largely dependent on the quality of the helical electron beam (HEB) formed by the magnetron-injection gun (MIG). Transition to the wavelengths $\lambda \approx 1$ mm and farther into the submillimeter-wave band requires allowing for additional physical factors in the process of analyzing

* manuilov@rf.unn.ru

[1] Institute of Applied Physics of the Russian Academy of Sciences, [2] N. I. Lobachevsky State University of Nizhny Novgorod, Nizhny Novgorod, Russia. Translated from Izvestiya Vysshikh Uchebnykh Zavedenii, Radiofizika, Vol. 59, No. 2, pp. 145–152, February 2016. Original article submitted December 25, 2014; accepted May 19, 2015.

HEBs theoretically and within the numerical model used to optimize MIGs. At the same time, specific features of this wavelength band were not allowed for within most numerical models used, and the calculations were performed by the method developed before for the MIGs of centimeter-wave gyrotrons. As a rule, this approach aims at achieving optimization with lower values of the pitch factor and does not allow one to obtain highly stable extreme output characteristics of the corresponding gyrotrons. In what follows, we illustrate specific features of calculating such systems on an example of calculating the electron-optical system (EOS) of a spectroscopic gyrotron having a frequency of 263 GHz and an output radiation power of several hundreds of watts. The optimized EOS is sufficiently universal and can be used successfully for spectroscopy employing gyrotrons operated at both 263 GHz and 526 GHz.

2. SPECIFIC FEATURES OF THE ELECTRON-OPTICAL SYSTEMS OF GYROTRONS OPERATED IN THE SHORT-WAVE PART OF THE MILLIMETER-WAVE BAND AND REQUIREMENTS FOR THE METHOD OF MODELING THEM NUMERICALLY

The range of requirements imposed on the gyrotron EOS is rather wide and, generally speaking, contradictory. As a rule, the following should be ensured:

1) a sufficiently high pitch factor, to ensure acceptable values of the efficiency and starting current;

2) moderate spread in electron velocities;

3) low coefficient of electron reflection from the magnetic mirror;

4) high electric strength;

5) low perturbations in the electron velocity distribution introduced by the electric field of the space charge of the beam;

6) technical effectiveness of the design;

7) moderate current density, to ensure a long lifetime of the emitter and, at the same time, no underheating of the cathode, which results in inhomogeneous emission of electrons and a greater spread of electron velocities.

It is becoming increasingly difficult to satisfy all the above-specified requirements, as the wavelength decreases and passes over to the short-wave part of the millimeter-wave band (in the case under consideration, the wavelength is $\lambda \approx 1.1$ mm). In particular, it follows from the formulas in the adiabatic MIG theory [7, 8] that under other equal conditions, the magnetic-field compression $\alpha = B_0/B_\mathrm{k}$, where B_0 and B_k are the magnetic fields in the operating space and at the emitter, respectively, increases with decreasing wavelength in accordance with the formula

$$\alpha \propto \lambda^{-2/3}. \tag{1}$$

As a result, the total length becomes longer, the magnetic field at the emitter decreases, and the height h of electron trajectories in the gun changes obeying the law $h \propto \lambda^{2/3}$. The latter factor leads to a sharp increase in the influence of the emitter roughness on the velocity distribution compared with the MIGs of the gyrotrons operated in the centimeter-wave band or the long-wave part of the millimeter-wave band [8, 9]. According to [9], the spread $\delta v_\perp$ of oscillatory velocities, which is determined by this factor, is specified by the formula

$$\delta v_\perp \propto (r_0/h)^{1/2} \propto r_0^{1/2}\lambda^{-1/3}, \tag{2}$$

where r_0 is the value of the emitter roughness. It is easy to evaluate that as one passes over from the centimeter-wave to the millimeter-wave band, the contribution of the roughness to the electron velocity spread grows by 2–3 times and becomes the main factor which determines the final spread of electron velocities at moderate beam currents. The contribution of the roughness exceeds even the influence of the field of the space charge of the beam, which usually determines the final spread of electron velocities and the limiting beam current [8]. This trend is confirmed by many experimental data and theoretical analysis [10, 11]. Therefore, the method of numerical analysis [12, 13], which allows for only the two-dimensional distribution of the electric field of the electrodes, the intrinsic Coulomb field of the beam and the magnetic field of the solenoids, can be used only for tentative optimization and identification of acceptable

TABLE 1. Main parameters of the gyrotron.

Operating frequency f, GHz	263.200
Magnetic field in the cavity B_0, T	9.578
Accelerating voltage U_0, kV	15.000
Beam current I_b, A	0.200
Cavity radius R_c, mm	2.537
Radius R_0 of the guiding center in the cavity, mm	0.960
Pitch factor g	1.300

MIG operation regimes. Additionally, it should be taken into account that MIGs are characterized by a mirror configuration of the magnetic field, which leads to partial reflection of the electron beam from the magnetic mirror when one tries to overcome a certain threshold value g_max of the average beam pitch factor. Elementary estimations show that

$$g_\mathrm{max} \approx (\delta v_\perp)^{-1/2}. \tag{3}$$

Substituting here the value of $\delta v_\perp$ from Eq. (2), we obtain the estimate

$$g_\mathrm{max} \propto \lambda^{1/6}. \tag{4}$$

This indicates that the maximum permissible pitch factor decreases gradually as the wavelength decreases, which has been confirmed by experimental data many times. Estimate (3) is found from the condition that the electrons having the maximum oscillatory velocity stay on the verge of reflection, i.e., their longitudinal velocity in the operating space is close to zero. Indeed, the value of g_max is slightly higher than the above-specified value and is determined by the maximum admissible value of the coefficient of reflection K_ref from the magnetic mirror. According to the available theoretical data [11, 14], if K_ref exceeds 2–3%, oscillations in the space charge and the processes of cathode bombardment and heating by reflected particles develop in the beam. Therefore, to ensure the beam stability, it is desirable to have such a pitch factor and width of the electron distribution function, at which the value of K_ref stays at least below 1%.

Thus, the standard MIG calculation method [12, 13] should be supplemented with an allowance for thermal electron velocities and the influence of roughness of the emitting surface for correct determination both of the electron velocity spread and of the evaluation of the beam stability on the basis of calculations of the coefficient of electron reflection from the magnetic mirror (see [15] for more details). All the above-specified features of analysis, optimization, and the requirements imposed on the numerical models of MIGs of subterahertz gyrotrons were allowed for in the theoretical EOS calculation which is presented below.

3. OPTIMIZATION OF THE ELECTRON-OPTICAL SYSTEM OF A GYROTRON OPERATED AT A FREQUENCY OF 263 GHz

A gyrotron with an operating frequency of 263 GHz is intended for operation in the continuous regime with a high stability of output parameters. To achieve a more flexible control over beam parameters, we chose a version of the MIG with the isolated first anode (the anode potential U_a can differ from the cavity potential U_0). The operation regime of the gun could vary between the diode and triode regimes with $U_\mathrm{a} \approx (0.7\text{–}1.0)U_0$. For convenience, the main parameters of the gyrotron are presented in Table 1 (the general gyrotron design concept is described in more detail in [16]).

The initial estimates of the MIG parameters were performed in accordance with the formulas of the adiabatic theory [7, 8] allowing for the above-specified restrictions and are presented in Table 2. To reduce the influence of the space charge field on the HEB parameters, the angle of emitter inclination to the gyrotron axis was chosen to be $\psi = 27^\circ$, so that MIG would form a quasi-laminary beam [13].

Then, the shapes of the cathode and the first MIG anode were varied within the model with zero initial electron velocities, in order to achieve a low position spread of electron velocities, an acceptable

TABLE 2. Main parameters of the magnetron-injection gun.

Magnetic-field compression α	26.6
Distance L_z between the emitter center and the center of the magnetic system, mm	354
Anode voltage U_a, kV	15
Electric field at the cathode E_k, kV/mm	4
Cathode radius R_k, mm	5
Anode-to-cathode gap d, mm	5
Emitter width L, mm	0.8
Current density j_k, A/cm^2	0.8

TABLE 3. Parameters of the beam calculated by using the model with zero initial velocities (the corresponding values have the index 0) and the model which allows for the combined influence of the initial thermal electron velocities and the emitter roughness. The nominal regime is $U_\mathrm{a} = U_0 = 15$ kV.

I_b, A	g_0	$\delta v_{\perp 0}$	g	$\delta v_\perp$	K_ref, %
0.00	1.366	0.0253	1.372	0.1770	0.23
0.05	1.359	0.0259	1.372	0.1742	0.27
0.10	1.351	0.0265	1.361	0.1775	0.27
0.15	1.341	0.0271	1.350	0.1808	0.27
0.20	1.339	0.0280	1.339	0.1841	0.27

electric strength (the field at any point in the EOS should not exceed 6 kV/mm), and the specified pitch factor. The corresponding method was described in more detail in [12, 15]. According to the calculation data (see Table 3), the spread of electron velocities in the optimized EOS version (Fig. 1) is still low and weakly dependent on the current at any permissible value of the latter.

It has already been stated that as one passes over to the subterahertz frequency band, the influence of the emitter roughness becomes a determining factor for evaluation of the HEB quality. Therefore, the final stage of numerical MIG analysis included a calculation of the electron distribution function in their oscillatory velocities (allowing for combined influence of the emitter roughness and the initial electron velocities), which served as the basis for determination of the coefficient of electron reflection from the magnetic mirror in order to evaluate the degree of HEB stability. The above-specified calculations were performed using the modified EPOS code which is described thoroughly in [10, 15]. Of the three components of the initial electron velocity (azimuthal v_θ, radial v_r, and axial v_z ones), the azimuthal component has the greatest influence on the rotational electron velocity in the operating space. Therefore, we allowed for this component of the initial electron velocity only, when modeling the combined influence of the thermal electron velocities and the emitter roughness numerically at the electron launch points. This component arises due to the action of a strong local electric field, which has a characteristic scale of tens of micrometers. The electron distribution function in v_θ was set to be close to the Gaussian one, since each of the mentioned factors yields the Gaussian distribution of electrons with respect to this value. The corresponding numerical data are presented in Table 3. The typical function $f(v_\perp)$ of electron distribution in oscillatory velocities is shown in Fig. 1. It stays close to the Gaussian one in the entire admissible current range, whereas the electron reflection coefficient is about an order of magnitude less than the threshold value, at which instabilities are formed in the HEB. This allows one to expect that a stable HEB will be formed in the operating regimes of the gyrotron.

Further studies of the MIG sensitivity to the bias in the magnetic field and small displacements of the cathode and anode off the calculated positions by $\pm(0.5$–$1.0)$ mm, which were caused by thermal expansion, demonstrated that the electron velocity spread is almost independent of the above-specified displacements,

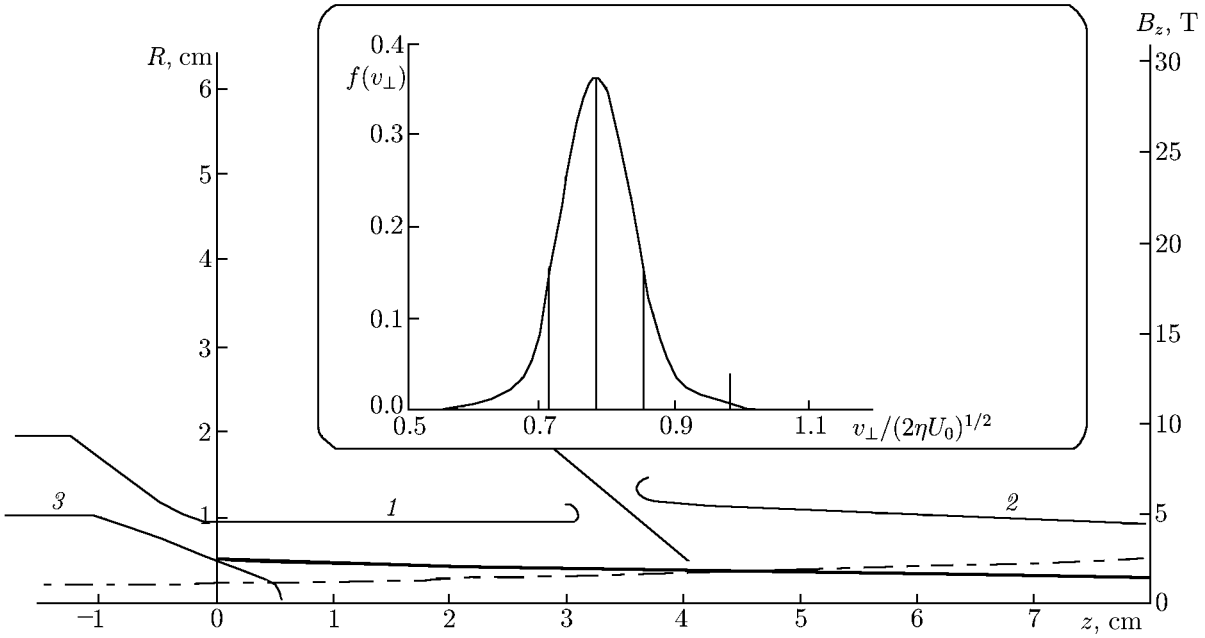

Fig. 1. Configuration of the electrodes of the optimized triode MIG (*1* is the first anode, *2* is the second anode, and *3* is the cathode) and the function of electron distribution over oscillatory velocities for a current of 0.2 A. Here, B_z is the longitudinal component of the magnetic field, z is the longitudinal coordinate, R is the radius, and η is the ratio of the charge and mass of the electron. Thin solid lines show the profiles of the electrodes, the thick line represents the electron beam, and the dash-dotted line is the longitudinal distribution of B_z.

and the electron pitch factor changes by no more than ± 0.1 of the calculated value. These changes agree with the predictions of the adiabatic theory perfectly. Calculations show that the optimized MIG allows one to fine-tune the power and frequency of the gyrotron efficiently, while retaining the HEB parameters in the acceptable range.

Further experimental studies of the gyrotron confirmed good HEB parameters in the calculated regimes completely and allowed us to achieve an efficiency of 17%, an output radiation power of 1 kW, and a frequency stability of $2 \cdot 10^{-6}$ (the results of the corresponding experiments will be published as a separate paper).

The electron-optical system should ensure scattering of the residual power of the electron beam over the collector surface. In what follows, we describe the choice of a simplest, cylindrical shape of the collector having a diameter of 20 mm. A distinctive feature of the EOS is the short distance between the beam and the system axis compared with characteristic radial dimensions of the coils of the superconducting cryomagnet. Therefore, the guiding field lines arrive at the collector surface at a very low angle, only 1.5°, which can result in a higher collector sensitivity to minor shifts of the cathode, which are caused by thermal expansion and axial misalignment of the magnetic system. Analysis of electron trajectories in the collector region for the no-generation case (the most difficult case from the viewpoint of the thermal load on the collector) showed that for a beam current of 0.1 A (the current at which most of the experimental gyrotron studies were performed, see [16]; the beam power was 1.5 kW), the start and end of the beam landing area are located in the cross sections $z = 534$ mm and $z = 571$ mm, respectively (the cross section $z = 0$ corresponds to the center of the cryogmagnet), and the peak power density amounts to 0.11 kW/cm^2 (see Fig. 2), which is quite acceptable. Estimates of the displacements of the beam landing area due to technological errors in the process of tube assembly and adjustment show that this region can deviate by 50 mm off the calculated position. Therefore, the collector cooling region was designed to a corresponding conservative tolerance. At a maximum calculated MIG current of 0.2 A, the collector load does not exceed 0.25 kW/cm^2, which is also fairly acceptable, and the trace beam shifts to the left insignificantly.

4. CONCLUSIONS

The electron-optical system of a gyrotron intended for spectroscopic studies and having an operating frequency of 263 GHz and an output radiation power of several hundreds of kilowatts has been developed. The magnetron-injection gun (MIG) was modeled numerically and optimized by using a sequence of analytical and numerical models, which made it possible to allow for the specific features of the subterahertz frequency band most adequately and, at the same time, to minimize the amount of computations in the process of optimization of the MIG geometry. At the first stage, we made preliminary estimates and chose the main parameters of the electron-optical system on the basis of the simplest adiabatic model of particle motion in the formation region. The second stage included numerical optimization of the MIG geometry and the electric regime on the basis of a model with zero initial electron velocities. In the process of optimization, we allowed for the influence of the electric field of the electrodes and the Coulomb field of the beam. Finally, the third stage of calculations was based on the most complete physical model, which, along with the above-specified factors, also allowed for the influence of the emitter roughness and thermal electron velocities. Allowance for the former factors is necessary to determine correctly the parameters of helical electron beams in submillimeter-wave gyrotrons and evaluate the degree of stability of these beams by calculating the coefficient of electron reflection from the magnetic mirror and the profile of the electron distribution functions in oscillatory velocities [17].

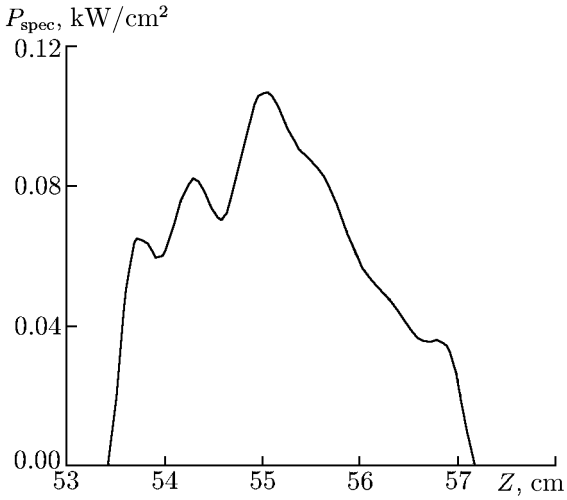

Fig. 2. Distribution of the power density over the collector surface in the non-generating gyrotron.

It is shown that a distinctive feature of gyrotrons for spectroscopic studies is low angles of beam incidence on the collector surface. This requires the widening of the operating area of collector cooling.

The developed electron-optical system allowed us to develop a gyrotron for spectroscopic studies operated at the main cyclotron resonance at a frequency of 263 GHz and a power of 100 W [16]. This system will be used to design the gyrotron operated at the second harmonic and an operating radiation power of 526 GHz.

The authors are grateful to M. Yu. Glyavin, V. E. Zapevalov, and A. V. Sedov for many useful discussions during the fulfillment of this work.

This work was supported by the Russian Science Foundation (project No. 14–12–00887).

REFERENCES

1. A. G. Litvak, G. G. Denisov, V. E. Myasnikov, et al., *Int. J. IRMM THz Waves*, **32**, No. 3, 337 (2011).
2. M. Yu. Glyavin, A. G. Luchinin, V. N. Manuilov, et al., *Radiophys. Quantum Electron.*, **54**, Nos. 8–9, 600 (2011).
3. V. L. Bratman, A. A. Bogdashov, G. G. Denisov, et al., *Int. J. IRMM THz Waves*, **33**, No. 7, 715 (2012).
4. J. H. Booske, R. J. Dobbs, C. D. Joye, et al., *IEEE Trans. Terahertz Sci. Technology*, **1**, No. 1, 54 (2011).
5. M. Thumm, *State-of-the-Art of High Power Gyro-Devices and Free Electron Masers*, KIT Scientific Publishing, Karlsruhe (2013).
6. M. Yu. Glyavin, G. G. Denisov, V. E. Zapevalov, et al., *J. Communi. Tech. Electron.*, **59**, No. 8, 792 (2014).

7. Sh. E. Tsimring, *Lectures on Microwave Electronics (3rd Winter Workshop for Engineers), Vol. 4* [in Russian], Saratov State Univ. (1974), p. 3.
8. Sh. E. Tsimring, *Introduction to High-Frequency Vacuum Electronics and Physics of Electron Beams* [in Russian], Inst. Appl. Phys., Nizhny Novgorod (2012).
9. Sh. E. Tsimring, *Radiophys. Quantum Electron.*, **15**, No. 8, 952 (1972).
10. V. K. Lygin, *Int. J. Infrared Millimeter Waves*, **16**, No. 2, 363 (1995).
11. A. N. Kuftin, V. K. Lygin, Sh. E. Tsimring, and V. E. Zapevalov, *Int. J. Electron.*, **72**, Nos. 5–6, 1145 (1992).
12. V. K. Lygin and Sh. E. Tsimring, *Zh. Tekh. Fiz.*, **43**, No. 8, 1695 (1973).
13. V. N. Manuilov and Sh. E. Tsimring, *Radiophys. Quantum Electron.*, **24**, No. 4, 338 (1981).
14. V. N. Manuilov and S. A. Polushkina, *Radiophys. Quantum Electron.*, **52**, No. 10, 714 (2009).
15. P. V. Krivosheev, V. K. Lygin, V. N. Manuilov, and Sh. E. Tsimring, *Int. J. Infrared Millimeter Waves*, **22**, No. 8, 1119 (2001).
16. M. Glyavin, A. Chirkov, G. Denisov, et al., *Proc. 9th Int. Workshop on Strong Microwaves and Terahertz waves: Sources and Applications, Nizhny Novgorod, Russia, July 24–30, 2014*, p. 203.
17. A. N. Kuftin, V. K. Lygin, V. N. Manuilov, et al., *Int. J. Infrared Millimeter Waves*, **20**, No. 3, 361 (1999).